SKELETON-BASED ANALYSIS OF BUTTERFLIES DERIVED BY COLOUR IMAGES

Giuliani Donatella
University of Bologna - Italy
giulianidonatella@libero.it

ABSTRACT

This paper presents a method to compute skeleton graph of butterflies extracted by colour images. This approach has been proved effective when applied to butterfly recognition, despite of their complex colour patterns and shapes. At first, we have decomposed a given coloured image into a group of contour parts, generating a binary segmented image. Secondly, we have analyzed the binary images containing bi-dimensional bounded shapes, generally not-simply connected. In order to do so, we have considered a generalized anisotropic flow for the evaluation of an external force field which will be applied on a parametric active contour procedure. Through the divergence we have investigated the field flow at different times noticing that the field divergence satisfies an anisotropic diffusion equation as well. Hence, it emerged that the curves of positive divergence can be considered as propagating fronts that converge to a steady state formed by shocks points. Using several natural shapes, we have proved that the sets of points inside the forms where divergence assumes positive values converge to the skeleton. This methodology has also been tested on shapes with boundary perturbations and disconnections.

Index Terms— Skeleton, medial axis, anisotropic flow, divergence flow

1. INTRODUCTION

This work investigates a new method for recognition of biological structures. Classification criteria often aim to research the basic morphological features and a typical approach to identify an unknown form is to measure morphological and metric attributes, such as positions of landmarks, size, extension, curvature, and so on. Instead, with this study we present an alternative methodology for butterfly recognition based on skeleton detection. Indeed, skeletons are frequently used as shape descriptors in biological species classification. The first step of our method consists in performing the segmentation of the initial colour image into regions, to find boundaries and the most significant areas which are frequently disconnected (Fig.1). In this way we produced a binary image with a shape not-simply connected in which we can distinguish the principal body components: head, thorax, abdomen, forewings and hindwings.
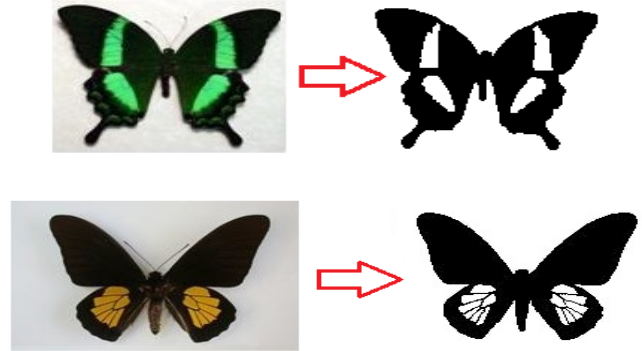

Fig. 1. Butterflies: Aureliana, Papilio Palinurus and Triodes Rhadamantus

Afterwards, we have applied a new approach for tracing skeleton of a given 2D bounded shape, which relies on divergence of an anisotropic vector field flow. To this aim, we have generated a vector force field for edge extraction through the resolution of a generalized parabolic equation, initialized to the gradient of an edge detector. Therefore, we have recourse to divergence in order to better analyze the field convergence. As the vector field varies over time, its divergence will change accordingly. Then, we focused our attention on its convergent behaviour since it will result essential to skeletonize the extracted contour. Indeed, the analysis of convergence is very helpful also for edge extraction because it allows to enclose regions from which the field flow has been originated and to position a suitable initial contour for shape reconstruction. This skeletonization method has a straightforward implementation and we have tested it with a wide set of 2D binary shapes, even if not closed or not-simply connected. Since this approach is able to analyze not-simply connected objects with irregular boundaries, it turns out to be suitable for processing natural and coloured images derived by real life.

2. SKELETONIZATION USING THE ANISOTROPIC DIVERGENCE FLOW

This study mainly deals with parametric deformable models. Within this scenario, edge detection is realized by a deformable process through active contours or surfaces, embedded on image domain, that move under the influence of internal and external forces [1],[2]. Internal forces are designed to smooth the model during deformation. External forces are computed from image data and are used to move the model towards the researched features [3], [4], [5]. We suggest that such external forces

$$\vec{F}_{Ext}(\vec{x}) = \vec{v}(\vec{x})$$

can result as solution of the following anisotropic diffusion equation [6]

$$\begin{cases} \vec{v}_t = div\big(g\big(|\nabla f|\big)\cdot \nabla \vec{v}\big) + \bar{F}(\vec{v}) \\ \vec{v}(x,y,0) = \vec{v}_0(x,y) = \nabla f \end{cases} \quad (1)$$

where div and ∇ are divergence and gradient operators respectively, g(.) is the diffusion coefficient. In this prototypical parabolic equation the initial condition ∇f is the gradient of an edge detector and $\bar{F}(\vec{v})$ is a forcing term for the diffusion process. The initial vector field ∇f is composed by vectors directed towards edges with norms significantly different from zero only in proximity of them. The diffusivity function g(.) is monotonically decreasing to zero, as a consequence, the vector flow will take place inside or outside the bounded region, and thus the shape contour will be a barrier for flow propagation. We refer to the force field generated by (1) as Anisotropic Vector Field (AVF) [7]. In this more general framework, we could consider the GGVF, the Generalized Gradient Vector Flow [8], as a special case of equation (1). Indeed we recall that the GGVF model satisfies the equation:

$$\vec{v}_t = g\big(|\nabla f|\big)\cdot \nabla^2 \vec{v} - h\big(|\nabla f|\big)\cdot(\vec{v} - \nabla f) \quad (2)$$

So, if we rewrite equation (1) as:

$$\vec{v}_t = \nabla g \cdot \nabla \vec{v} + g\nabla^2 \vec{v} + \bar{F}(\vec{v})$$

we derive the GGVF field assuming:

$$\nabla g \cdot \nabla \vec{v} = 0 \qquad \bar{F}(\vec{v}) = -h\big(|\nabla f|\big)\cdot(\vec{v} - \nabla f)$$

where $h(\cdot) = 1 - g(\cdot)$ is a monotonically decreasing function. The source term considered in the GGVF model does not produce a significant contribution, because it tends to zero both near edges, due to the chosen initial conditions, as well as far from them, since the function h(.) is decreasing. If we take into account a source term significantly different from zero, such as:

$$\bar{F}(\vec{v}) = g_0\big(|\nabla f|\big)\cdot(\vec{v} - \nabla f) \qquad g_0\big(|\nabla f|\big) = b \cdot e^{-c|\nabla f|^a}$$
$$b \geq 1, c > 0, 0 < a \leq 1$$

the convergence of the diffusion process will get faster since this source term is approximately null near edges but it increases as moving away from them [6],[7]. To avoid the effects of the initialization problem [9],[10],[11] we suggest to study the basic structure of the field through its divergence, which is a measure of field convergence at a given point. In order to do so, we have evaluated the *divergence map* associated to the field, that is a grayscale image depicting divergence values [12]. This map is characterized by a gray background with divergence values almost zero, black curves with negative divergence in correspondence to edges and a set of light curves with positive values, defining regions from which the vector field comes out. The divergence map will guide us in the choice of shape and position of an appropriate initial contour. The evolving curve will fit well into the final edge [12] only if any selected initial contour encloses completely the regions from which the field flows.

2.1. Flow of divergence and skeletonization

As the divergence operator is applied to a vector field varying on time, the related divergence map is varying as well. In Fig.2 we show the divergence maps of a fish realized using the AVF vector field at different times.
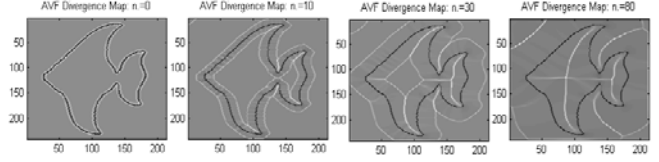

Fig. 2. Divergence Maps with different numbers of iteration

As we can see, the curves of positive divergence gradually flow from edges inside and outside the bounded shape. In addition, we can analytically prove that also the field divergence satisfies a diffusion equation [12]. The curves of positive divergence can be considered as propagating fronts of the evolution function $\varphi = div(\vec{v})$. The set of points in the image domain where the function φ assumes positive values correspond to the position of a propagating interface. We called these curves *positive-valued sets* [12]. Specifically given an image $I(x, y)$, let C be the object considered for edge extraction with boundary ∂C. We distinguish the positive-valued sets in the interior of the shape C from those outside:

$$\varphi_{Int}^+ = \{\vec{x} \in C \setminus \partial C : \varphi(\vec{x}) = div(\vec{x}) > 0\}$$
$$\varphi_{Ext}^+ = \{\vec{x} \in I \setminus C : \varphi(\vec{x}) = div(\vec{x}) > 0\}$$

These will be defined as *internal positive-valued sets* and *external positive-valued sets,* respectively. At the end of the flow process, the evolving curve φ_{Int}^+ converges to an equilibrium configuration forming the skeleton of the shape, as shown in the test image reproducing a butterfly (Fig.3).
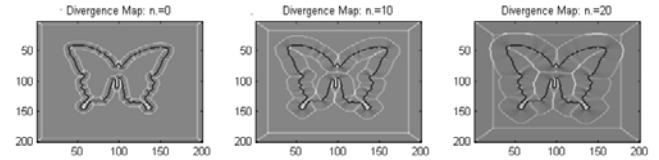

Fig. 3. Divergence Maps of a butterfly with different iteration numbers

Between the several equivalent definitions of skeleton for bi-dimensional shapes [13],[14], one of them describes this notion through the grass fire model. According to this theory, all points along the object boundary are simultaneously set on fire, flames propagate both inside and outside the region, and the skeleton points are located where the internal evolving fronts meet themselves. According to the Huygens Principle, the skeleton points are the shocks that appear during propagation.
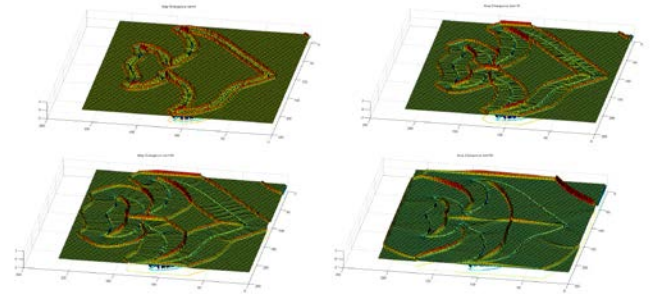

Fig. 4. 3D representation of propagating fronts with positive divergence

By a careful analysis of divergence maps, we notice that the contour with negative divergence values does not move, whereas the sets φ_{Int}^+ and φ_{Ext}^+ can be thought as wave fronts propagating

inside and outside C. We assume that the stationary configuration of the internal positive-valued sets gives rise to the skeleton, named *internal skeleton*, whereas the external positive-valued sets form a sort of *external skeleton.* In the three-dimensional graphs of Fig.4, we clearly see that the skeleton is the loci where the propagation fronts φ_{Int}^+ collide with each other, without crossing.

Once the steady state has been reached, the identification of shock points is straightforward because the evolving surface changes sharply from null to positive values in correspondence to them. Applying this skeletonization method to the not-simply connected shape of Fig.5, we observe that the divergence flow generates wave fronts propagating inside the white circular forms. Their skeleton curves collapse in a point for the small circle and in a segment for the ellipse. In the meantime, the external positive-valued sets of the white holes flow towards the internal positive-valued set of the black rectangle, and at the end, they collide without crossing. In this way the steady configuration of the diffusion process gives rise simultaneously to the skeleton of the white holes and of the background region, not-simply connected.
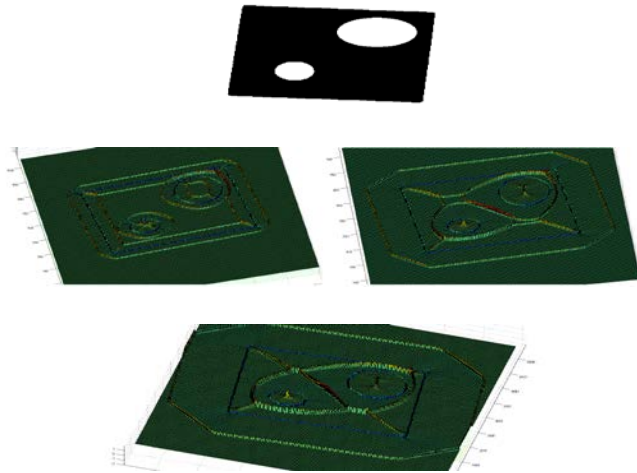

Fig. 5.   Propagating fronts of divergence for a not-simply connected shape

According to another definition, the skeleton or medial axis [15],[16],[17] is described as the locus of the centres of all maximal inscribed circles. We could note that the positive-valued sets φ_{Int}^+, related to the steady state of divergence flow, satisfy this defining property: to any skeleton point corresponds at least two boundary points. In Fig.6 and Fig.7 we show the divergence maps and some maximal inscribed circles for the rectangle with two holes of Fig.5, and for the butterflies Papilio Palinurus and Aureliana, respectively.
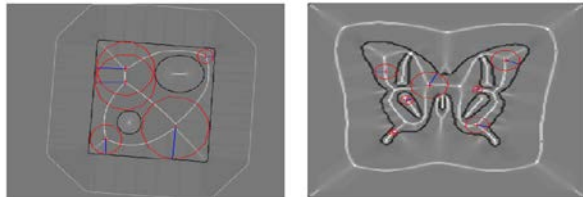

Fig. 6.   Skeleton: locus of centres of maximal inscribed circles

Fig. 7.   Skeleton: locus of centres of maximal inscribed circles

Another approach for medial axis detection is based on distance transform values [18], [19] [20] [21], which specify the distance of each point to the closest boundary. The skeleton is described as being the *locus of local maxima,* or *ridges,* on the distance transform. However, the detection of skeleton points as gradient singularities of DT is difficult and numerically unstable [22],[23],[24]. Through the steady configuration of divergence, skeleton extraction can be performed in a simplified way because its points do not correspond to discontinuities of the first order derivatives of a distance function, but to discontinuities of the divergence function itself, $\varphi = div(\vec{v})$. In addition, the detection of these singularities is directly performed because the divergence map's intensities are significantly different from zero only in correspondence of the boundary, the external skeleton and the internal one, where they result negative and positive respectively. The skeleton curves lie along the discontinuities of the evolution function φ that passes abruptly from null to positive values. These features are clearly evident through the three-dimensional plot of the function $\varphi = div(\vec{v})$ related to a rectangular shape (Fig.8).
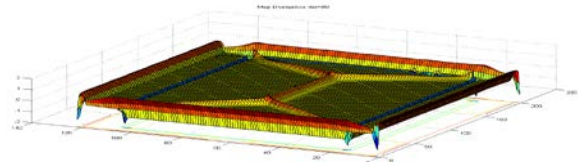

Fig. 8.   Skeleton of a rectangular form: branches and junction points

Furthermore it emerged that the local maxima of the function φ_{Int}^+ correspond to the junction points of the skeleton branches. Indeed, three wave fronts coming from consecutive sides meet and merge in each of the two junction points. According to the superposition principle, their intensities add up reaching local maxima (Fig.8).

2.2. Properties of Skeletonization using divergence flow

With regard to the uniqueness of the skeletonization process, we could verify that the skeletons of the two shapes in Fig.9 are very similar.
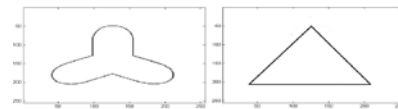

Fig. 9.   Not-convex and triangular forms

The comparison of Fig.10 and Fig.11 leads us to conclude that the not-convex shape and the triangle have the same internal positive-valued sets φ_{Int}^+ whereas the sets of points φ_{Ext}^+ are totally different. Therefore the uniqueness of skeleton will be

ensured only if both sets φ_{Int}^{+} and φ_{Ext}^{+} are considered. We assume that two forms have the same shape and hence belong to the same equivalence class, if and only if both sets φ_{Int}^{+} and φ_{Ext}^{+} are equivalent, except for similarity transformations.
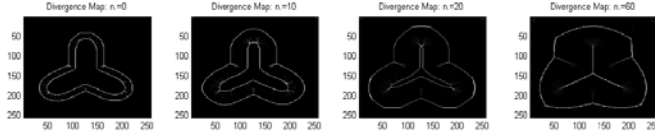

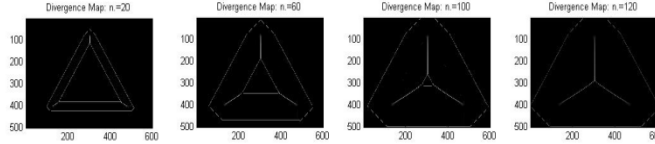Fig. 10. Evolution of positive-valued sets for a non-convex form

Fig. 11. Evolution of positive-valued sets for a triangular form

Now we address the well-known problem of any skeletonization method that is the intrinsic sensitivity to even small boundary variations [24]. To this regard, we have investigated the features of skeleton in presence of boundary perturbations of different level and outlines, as those displayed in Fig.12. Observing the three-dimensional representation of the divergence map, we can highlight significant differences in the profiles of branches generated by divergence flow with an increasing level of perturbations (see the right-hand side of Fig.12).
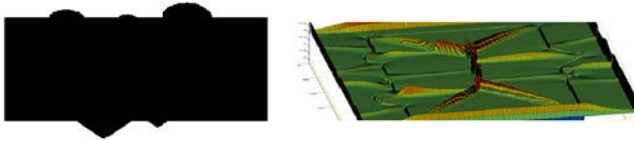

Fig. 12. 3D Divergence Map of a shape with boundary perturbations of different degree

The areas of the region bounded by the corresponding profiles will be very different as well. These areas will provide a quantitative measure for the level of irregularities and their values are strictly related to the magnitude of protuberances. With regard to the ability to reconstruct the original object from skeleton, we know that the medial axis, with the associated distance values, defines the medial axis transform or MAT, which is a complete shape descriptor because it can be used to recover the original form [24],[25],[26]. An object can be entirely reconstructed by computing the union of maximal inscribed balls with radii specified by the distance function values. Using this approach the original shape can be restored through the medial axis points detected recurring to the extraction of the positive-valued sets φ_{Int}^{+} as the steady configuration has been reached. To this aim, we have evaluated the level sets of the divergence function related to this field state. From isolines of the divergence's map contour we have automatically selected the curve that encloses the skeleton [6], which will be called *skeleton contour*. With this term we refer to the minimal closed curve which contains the skeleton. In this way the original shape can be reconstructed by selecting such curve as initial contour for the deformation process. By means a backward procedure, the original shape can be exactly restored through the vector field previously calculated. In Fig.13, as a demonstrative example, we have applied this procedure to the not-simply connected object of Fig.5.
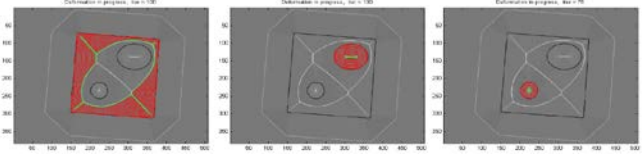

Fig. 13. Skeleton-contours and shape reconstruction

3. SKELETON-BASED ANALYSIS

The present skeletonization method captures intrinsic shape information about objects and it can be successfully used to shape matching and classification on silhouettes derived by natural images, as those of Fig.1. In order to do so, firstly we have evaluated the steady configuration of the internal positive-valued sets φ_{Int}^{+}. Then, we have generated a two-level maps (Fig.14) from which we have extracted the fore mentioned *skeleton contours*. The skeleton contour is a one-dimensional differentiable manifold that can be used as a shape descriptor in biological species analysis and recognition.
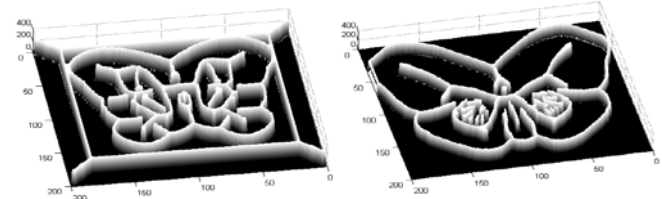

Fig. 14. Representation of positive-valued sets of Papilio Palinurus and Triodes Rhadamantus butterflies

The following figures (Fig.15,16,17) represent the extracted skelton contours of butterfly wings and of their coloured internal parts. The graphs below, show the evaluation of the angles $\theta(s)$ of tangent vectors versus a normalized curvilinear abscissa, computed for the corresponding skeleton sections. The blue circles are the initial points selected for the analysis of each curve. Through the tangent vectors we carry out a skeleton representation that is invariant for affine transformations. We notice that the internal skeleton contour of the principal body part is characterized by a strong axial symmetry. As we can see in Fig.18, the *external skeleton* pinpoints sections with high curvatures and consequently it enables to identify landmarks. In addition it can be selected as initial contour for restoring the original shape.
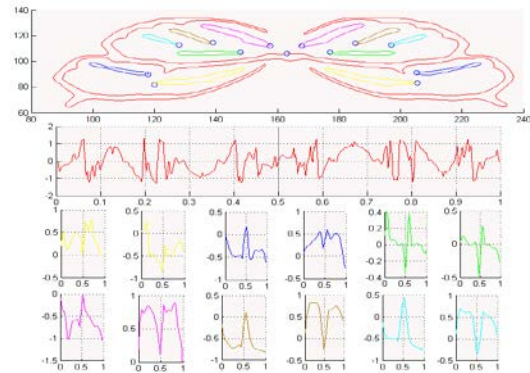

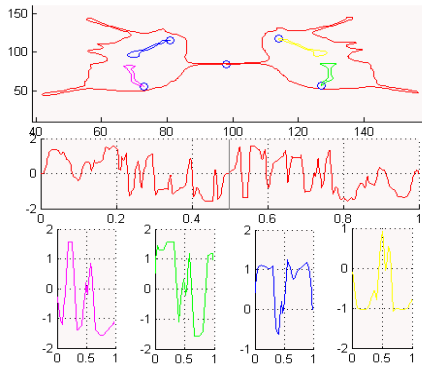Fig. 15. Skeleton-contours and angles θ(s) of tangent vectors (Aureliana)

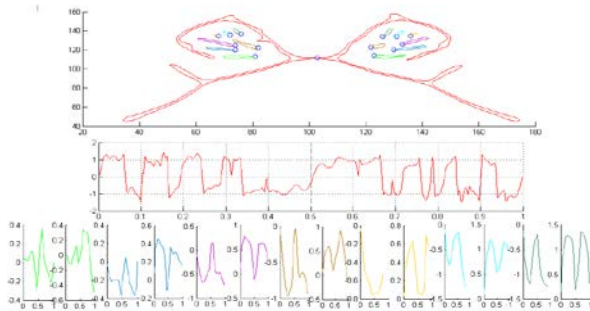Fig. 16. Skeleton-contours and angles θ(s) of tangent vectors (Papilio Palinurus)

Fig. 17. Skeleton-contours and angles θ(s) of tangent vectors (Triodes Rhadamantus)

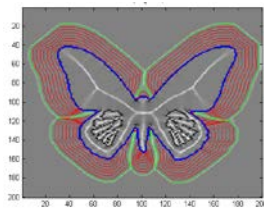
Fig. 18. Shape recontruction of Triodes Rhadamantus using external skeleton

REFERENCES

[1] M. Kass, A. Witkin, D. Terzopoulos, "Snakes: active contour models" , *Int. Jour. Comp. Vision*, Vol. I, N.4, pp 321-331, 1988.

[2] C. Xu, L.J. Prince, "Snakes, shapes, and gradient vector flow", *IEEE Trans. on Image Processing*, 7, 1998

[3] B. Li, T.A Scott, "Active contour external force using vector field convolution for image segmentation",. *IEEE Transactions on Image Processing*, 16, pp 2096-2106, 2007.

[4] A. Kovács, T. Szirányi, "Improved force field for vector field convolution method", ICIP IEEE, pp. 2909-2912, 2011.

[5] C. Xu, L.J. Prince, "Gradient Vector Flow: a New External Force for Snakes", *IEEE Proc. Conf. on Comp. Vis. Patt. Recogn.*, CVPR'97, 1997

[6] D. Giuliani, "Edge Extraction with an Anisotropic Vector Field using Divergence Map", *International Journal of Image Processing (IJIP)*, Volume 6, Issue 4, 2012.

[7] D. Giuliani, "Edge Detection from MRI and DTI Images with an Anisotropic Vector Field Flow using Divergence Map", *Algorithms*, Special Issues "Machine Learning for Medical Imaging 2012", Vol.5 Issue 4, pp. 636-653, 2012.

[8] C. Xu, L.J. Prince, "Generalized gradient vector flow external forces for active contours", *Signal Proc., an Intern. Journal*, 71, 1998

[9] C. Li; J. Li; M.D. Fox "Segmentation of Edge Preserving Gradient Vector Flow: an Approach Toward Automatically Initializing and Splitting of Snakes". *IEEE Proc. Conf. on Comp. Vis. Patt. Recogn.*, CVPR'05, 2005.

[10] C.Tauber, H. Batiata,,A. Ayache "A Robust Active Initialization and Gradient Vector Flow for Ultrasound Image Segmentation", MVA2005 IAPR Conf. on Machine Vision Applications, 2005

[11] F. Yabin, L. Caixia, Z. Bingsen, P. Zhenkuan "An Improved Algorithm of Contour Initialization in Active Contour Model". *Image and Graphics*, ICIG,2007

[12] D. Giuliani, "Skeletonization using the Divergence of an Anisotropic Vector Field Flow", *IEEE Proc. Conf. on Applied Imagery and Pattern Recognition,* 2013.

[13] N. Cornea, D. Silver, P. Min, "Curve-skeleton properties, applications, and algorithms", IEEE TVCG 13,3 pp 87-95, 2007.

[14] R. Càrdenes ,J. Ruiz-Alzola., "Skeleton extraction of 2D objects using shock wavefront detection" , Computer- Aided Systems Theory-EURCAST 2005, Volume 3643, pp 392-397, 2005.

[15] H. Blum , "A transformation for extracting new descriptors of shape", *Models for the Perception of Speech an Visual Form,* ex W. Whaten-Dunn Ed., MIT Press, Cambridge, MA, pp 362-380, 1967.

[16] H. Blum ."Biological shape and visual science". *J. Theoretical Biology*, 38, pp 205–287, 1973.

[17] Blum H., Nagel R.,"Shape description using weighted symmetric axis features", *Pattern Recognition,*10, pp 167-180, 1978.

[18] Montanari U., "A method for obtaining skeletons using a quasi-Euclidean distance", *Journal of* ACM ,16 (4), pp 534-549, 1969

[19] Siddiqi K., Bouix S., Tannenbaum A., Zucker S.W., "The Hamilton-Jacobi skeleton", *Proc*. ICCV (Corfù), pp 828-834,1999

[20] Katz R.A., Pizer S.M., "Untangling the Blum Medial Axis Transform", IJCV Special Issue UNC-MIDAG, 55 (2), pp 139-153,2003

[21] Bouix S.,Siddiqi K., "Divergence-based Medial Surfaces", Proc. ECCV 2000, pp 603-618, 2000

[22] Macrini D., Siddiqi K., Dickinson S., "From skeletons to bone graphs: Medial abstraction for object recognition", *CVPR*, 2008.

[23] S. Bouix ,K. Siddiqi, A. Tannenbaum, "Flux driven automatic centreline extraction", *Medical Image Analysis*, 9, pp 209-221, 2005

[24] M. Rumpf , A.Telea, "A continuous skeletonization method based on level sets", IEEE TCVG *Symposium on Visualization*, pp 362-380,2002

[25] F. Demirci, A.Shokoufandeh , S. Dickinson, " Skeletal shape abstraction from examples". *IEEE Tran. on PAMI*, 2009.

[26] L. Liu, E.W. Chambers, D. Letscher ,T. Ju,"Extended Grassfire Transform on medial axes of 2D shape", *J. Computer-Aided Design*,Vol.3, Issue 11,2011.